Advances in Water Resources 000 (2015) 1–11

Contents lists available at ScienceDirect

Advances in Water Resources

journal homepage: www.elsevier.com/locate/advwatres

Reading the signatures of biologic–geomorphic feedbacks in salt-marsh landscapes

Andrea D'Alpaos [a,*], Marco Marani [b,c]

[a] Department of Geosciences, University of Padova, Via Gradenigo 6, 35131 Padova, Italy
[b] Department ICEA, University of Padova, Via Loredan 20, 35131 Padova, Italy
[c] Division of Earth and Ocean Sciences, Nicholas School of the Environment and Department of Civil and Environmental Engineering, Pratt School of Engineering, Duke University, Durham, NC 27708, United States

ARTICLE INFO

Article history:
Available online xxx

Keywords:
Salt marshes
Vegetation
Biomorphodynamics

ABSTRACT

How do interacting physical and biological processes control the form and evolution of salt-marsh landscapes? Salt marshes are shaped by the erosion, transport and deposition of sediment, all of which are mediated by vegetation. In addition, vegetation plays a key role in deposition of organic material within marsh sediments. The influence of biota on salt-marsh landscapes is indeed well established. However, a fascinating and relevant question is whether one can identify the signatures of the underlying and intertwined physical and biological processes in marsh landscapes, and indeed infer from them the dynamic behavior of these coupled physical and biological systems. Can one detect landscape features that would not have emerged in the absence of interactions and feedbacks between physical and biological processes?

Here we use field evidence and a two-dimensional biomorphodynamic model to show that the interplay between physical and biological processes generates striking biological and morphological patterns. One such pattern, vegetation zonation, consists of a mosaic of vegetation patches, of approximately uniform composition, displaying sharp transitions in the presence of extremely small topographic gradients. The model describes the mutual interaction and adjustment between tidal flows, sediment transport, morphology, and vegetation distribution, thus allowing us to study the biomorphodynamic evolution of salt-marsh platforms. A number of different scenarios were modelled to analyze the changes induced in bio-geomorphic patterns by varying environmental forcings, such as the rate of relative sea level rise (RSLR) andsediment supply (SS), and by plant species with different characteristics. Model results show how marsh responses to changes in forcings are highly spatially dependent: while changes in SS most directly affect marsh areas closest to the channels, changes in the rate of RSLR affect the marsh platform as a whole. Organic sediment accretion is very important for allowing marshes to compete with increasing rates of RSLR near watershed divides, whereas inorganic sedimentation is more important closer to the channels. Increasing sediment supply to coastal marshes, therefore, might not compensate for rising sea levels, particularly in the inner marsh portions. Model results also emphasize that biodiversity is strongly controlled by environmental forcings and that zonation patterns are a signature of bio-geomorphic feedbacks with vegetation acting as a landscape constructor which feeds back on, directly alters, and contributes to shape tidal environments. Finally, the model generates realistic frequency distributions of vegetation occurrence, which nicely meet observed ones.

1. Introduction

When you stand on a salt-marsh platform and look across the marsh landscape can you see the signatures of the feedbacks between physical and biological processes? Whether or not we can unravel the signs and effects of the mutual interactions and adjustments between water fluxes, sediment transport, and vegetation dynamics is an important and fascinating question [53,60,63,75], which, however, has remained rather unexplored [18]. In the case of salt-marsh landscapes the issue is relevant also because salt marshes provide a substantial ecological and economic value: They provide a significant part of coastal primary production, are characterized by high biodiversity, and deliver valuable ecosystem services [7,42,77]. Salt marshes, in fact, dissipate waves and mitigate erosion during storms (e.g., [24,45,46,70]), mediate sediment and nutrient fluxes between terrestrial and marine systems (e.g., [7,28]), provide habitat for a variety of coastal biota (e.g., [58]), and serve as a sink for organic carbon

* Corresponding author. Tel.: +390498279117; fax: +390498279134.
E-mail address: andrea.dalpaos@unipd.it (A. D'Alpaos).

http://dx.doi.org/10.1016/j.advwatres.2015.09.004
0309-1708/

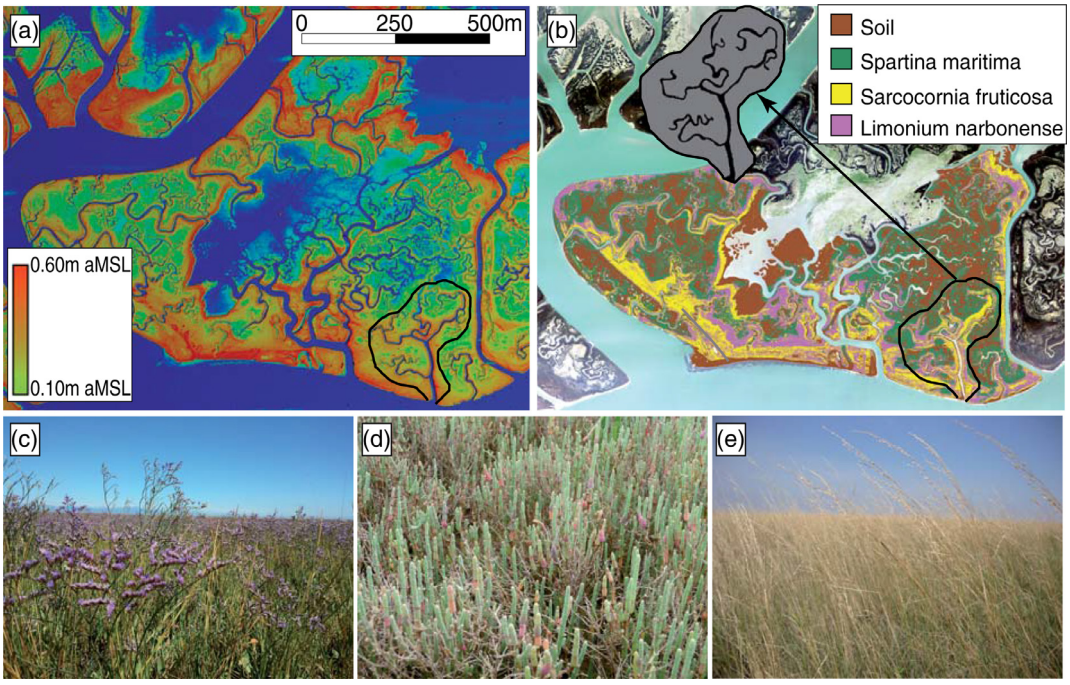

Fig. 1. (a) Color-coded topography of the San Felice salt marsh in the Venice Lagoon obtained from a LiDAR survey [72]. Higher elevations are coded in red and lower elevations in shades of blue. (b) Vegetation map of the San Felice salt marsh overlapped to the true-color representation of the multispectral remote sensing image (resolution = 0.5 m) from which it was created [37,72]. The typical patchy distribution associated to the zonation phenomenon of different vegetation types, namely *Limonium narbonense, Sarcocornia fruticosa*, and *Spartina maritima* is shown. The inset shows an actual watershed divide and the embedded channel network (see [35] for a detailed description of the study site and of the procedure used to delineate the watershed divide) used as model domain for the numerical simulations. (c)–(e) Samples of observed vegetation patches from salt marshes in the Venice lagoon: (c) *L. narbonense*, (d) *S. fruticosa*, and (e) *S. maritima*. (For interpretation of the references to color in this figure legend, the reader is referred to the web version of this article.)

(e.g., [6,22,26,40]). Despite the ecological and economic value of salt marshes, these ecosystems are being lost at critical rates threatened by increasing rates of relative sea level rise (RSLR) and limited sediment supply (SS) (e.g., [14,16,23,25,29,34,49]).

To understand how salt-marsh surfaces form, persist, drown or expand as a result of changes in environmental forcing (such as e.g., RSLR and SS) the delicate balance and feedbacks between morphology, hydrodynamics, sediment transport, and vegetation dynamics need to be explored and understood. Halophytic vegetation influences marsh hydrodynamics and sediment transport through increased inorganic sedimentation rates, due to an increased flow resistance and the reduction in turbulent kinetic energy, as well as through direct particle capture by plant stems (e.g., [30,50,67,71,74]). In addition, halophytes are known to enhance vertical accretion of marsh platforms through direct organic accumulation (e.g., [48,52,54,55]). Finally, halophytes improve the aeration of the soil, in the proximity of their roots, and induce an aerated layer that persists in the shallow subsurface despite frequent, regular flooding, with relevant implications for vegetation spatial distribution and related biogeomorphic interactions (e.g., [4,9,36,43,76]).

Over the past decades, mathematical modelling has become a relevant tool to describe the morphology and evolution of salt-marsh ecosystems (e.g., [21]). A number of bio-morphodynamic models, accounting for feedbacks between hydrodynamic processes, sediment transport and salt-marsh topography, mediated by vegetation presence and dynamics, have been developed. These models range from point (e.g., [2,11,14,33,34,38,47,48,52]), to one-dimensional (e.g., [32,39,51,66]), to two-dimensional (e.g., [3,12,27,68], and usually assume vegetation biomass to be at all times in equilibrium with the current soil elevation (with the exception of Marani et al. [34]). The above models have emphasized that the feedbacks among physical and biological processes are crucial for salt-marsh formation, presence, and continued existence, as well as in determining their responses to changes in environmental forcings. Hence, one may now wonder if the presence of two-way bio-geomorphic feedbacks can be fingerprinted and characteristic signatures of bio-geomorphodynamic processes can be identified in the marsh landscape. For example, salt-marsh landscapes are characterized by striking and widely-occurring zonation patterns, consisting in a mosaic of vegetation patches, of approximately uniform composition, exhibiting sharp spatial boundaries (e.g., [1,5,31,44,56,64,76]). The analysis of the frequency distribution of marsh species with soil elevation shows that halophytes are associated with narrow ranges of soil topographic elevations (e.g., [64,32]), and that there is a strong correlation between patterns in elevation and vegetation; an example is shown in Fig. 1, which portrays a color coded topography of the San Felice salt marsh in the Venice Lagoon (Fig. 1a), a vegetation map overlapped to a remote sensing image of the same marsh (Fig. 1b), and a few samples of observed zonation patches (Fig. 1c–e). Marani et al. [32] and Da Lio et al. [8] recently demonstrated that zonation patterns such as those in Fig. 1b indeed emerge from two-way feedbacks between biomass production and soil accretion, and that vegetation species actively tune soil elevation to maintain it within ranges of optimal adaptation. The observed patchy geomorphological–biological features (see Fig. 1 and [8,32]) are, in essence, the manifestation of multiple stable states, generated by competing vegetation species adapted to different elevation ranges.

Here we combine the hydrodynamic/sediment transport formulation of D'Alpaos et al. [12] and the coupled geomorphic-ecological framework of Marani et al. [32] to explore marsh eco-morphodynamics in a fully two-dimensional setting. This new, and realistic, 2D formulation allows us to compare the characteristics of eco-geomorphic patterns with observed ones, thereby testing hypotheses on the dynamic origin of zonation, to evaluate salt-marsh responses to environmental change (such as changes in the rate of RSLR and SS), and to study the role of vegetation characteristics

Please cite this article as: A. D'Alpaos, M. Marani, Reading the signatures of biologic–geomorphic feedbacks in salt-marsh landscapes, Advances in Water Resources (2015), http://dx.doi.org/10.1016/j.advwatres.2015.09.004

and of the tidal network structure in defining bio-geomorphic patterns.

2. Methods

We use here the approach proposed by D'Alpaos et al. [12] to describe tidal hydrodynamics and inorganic sediment transport, and couple it to vegetation competition and organic soil production as described by Marani et al. [32] and Da Lio et al. [8]. A basic description of the models is provided below; the reader is referred to the original papers for full derivations.

The two-dimensional depth-averaged hydrodynamic flow field is described through a simplified version of the shallow water equations [35,61], modified to account for wetting and drying processes over the marsh surface [12,15]. The model assumes an instantaneous propagation of the tide through the tidal network dissecting the marsh, whereas a balance between water surface slope and friction is assumed for the flow over the platform. The model is suitable to describe flow fields in relatively short tidal basins for which the spatial variations in water surface elevation above the platform are much smaller than the average water depth, as typically occurs over microtidal salt-marsh platforms. The marsh surface is also assumed to be nearly flat, with a constant dissipation in space and time (see [35,61] for a detailed description of the model and of the embedded assumptions). Water levels and flow velocities obtained under these hypotheses are subsequently used to model the transport and deposition of suspended sediments through an advection–dispersion equation:

$$\frac{\partial (CD)}{\partial t} + \nabla \cdot (\mathbf{U}CD - k_d D \nabla C) = Q_e - Q_d, \tag{1}$$

where $D(\mathbf{x}, t)$ is the local water depth (at site $\mathbf{x}$ in a planar Cartesian reference frame, at time t), $C(\mathbf{x}, t)$ is the local instantaneous depth-averaged suspended sediment concentration (hereinafter SSC), $\mathbf{U}$ is the local depth-averaged flow velocity field, $k_d = 0.3\ \mathrm{m^2\,s^{-1}}$ is the dispersion coefficient which accounts for dispersive effects associated with vertical variations in both flow velocity and sediment concentration, $Q_e(\mathbf{x}, t)$ and $Q_d(\mathbf{x}, t)$ are the local erosion and sedimentation fluxes, respectively (and represent sediment volume exchange rates per unit area between the water column and the marsh surface). The advection–diffusion equation is solved by imposing a fixed SSC, C_0, throughout the channel network. C_0 is assumed to be constant in space and time, and represents the external (fluvial and/or marine) inorganic sediment supply.

The temporal evolution of local bed elevations $z(\mathbf{x}, t)$ (computed with respect to mean sea level, hereinafter MSL) is governed by the sediment mass balance equation

$$\frac{\partial z}{\partial t} = Q_d - Q_e - R, \tag{2}$$

where R is the rate of relative sea level rise (RSLR) (i.e. the algebraic sum of SLR and local subsidence). The total sedimentation flux (Q_d) is the sum of the local inorganic deposition fluxes due to sediment settling (Q_s), direct particle capture by plants (Q_c), and of the local organic soil production (Q_o) mainly associated with below-ground biomass production.

By assuming a mutually exclusive erosion and deposition, the settling and the erosion fluxes are estimated through the empirical relationships proposed by Mehta [41] and Einstein and Krone [19]:

$$Q_e = \frac{Q_{e_0}}{\rho_b}\left(\frac{\tau}{\tau_e} - 1\right)\mathcal{H}(\tau - \tau_e), \tag{3}$$

$$Q_d = w_s \frac{C}{\rho_b}\left(1 - \frac{\tau}{\tau_d}\right)\mathcal{H}(\tau_d - \tau), \tag{4}$$

where $Q_{e0} = 5.0 \times 10^{-4}\ \mathrm{kg\,m^{-1}\,s^{-1}}$ is an empirical erosion rate [41], $\rho_b = (1-p)\rho_s$ is sediment bulk density after compaction has taken place, $p = 0.4$ and $\rho_s = 2650\ \mathrm{kg\,m^{-3}}$ are sediment bed porosity and density, respectively; τ is the magnitude of the local bottom shear stress (evaluated through the hydrodynamic model [61]); $\tau_e = 0.4\ \mathrm{N\,m^{-2}}$ and $\tau_d = 0.1\ \mathrm{N\,m^{-2}}$ are the threshold shear stresses for erosion and deposition, respectively, typical of cohesive sediment; $w_s = 1 \times 10^{-4}\ \mathrm{m\,s^{-1}}$ is sediment settling velocity for silt; and $\mathcal{H}$ is the Heaviside step function, which is zero for negative arguments and 1 for positive arguments.

The inorganic sedimentation flux due to particle capture by plants (Q_c) and the organic accretion rate (Q_o) depend on local plant biomass, B, which is in turn assumed to be at all times in equilibrium with the local current soil elevation, i.e. $B = B\,[z(\mathbf{x}, t)]$, on the basis of an "equilibrium vegetation model" [33,34] according to which annual vegetation productivity can adjust over a much faster timescale than the evolution of marsh surface elevation. In their original formulation, D'Alpaos et al. [12] considered the cases of (i) a scenario featuring one species of vegetation with biomass linearly decreasing with soil elevation between MSL and mean high water level (MHWL), and (ii) multiple vegetation species for which, as a result of competition and individual species adaptations, biomass production linearly increases with soil elevation between MSL and MHWL. The first scenario broadly mimics that of *Spartina* spp. dominated marshes in North America whereas the later broadly mimics the situation in the Venice Lagoon. In such a formulation, however, species competition, and its implications for organic soil production, is not explicitly modelled. We therefore follow here the approach proposed by Marani et al. [32], who consider a set of competing vegetation species, each adapted to different ranges of elevation, the latter assumed to effectively represent the combined effects of environmental stressors, such as soil hypoxia and salinity concentration. The surface accretion contribution associated with inorganic sediment interception by plants, $Q_c(\mathbf{x}, t)$, and with organic soil production, $Q_o(\mathbf{x}, t)$, can therefore be computed as

$$Q_c = \frac{C}{\rho_b}\,\alpha\, B_i^{\beta}\, U^{\gamma}, \tag{5}$$

$$Q_o = Q_{o_0} B_i, \tag{6}$$

where $\alpha = 1.02 \times 10^6 d_{50}^2 (\mathrm{m/s})^{1-\gamma} (\mathrm{m^2/g})^{\beta}$, $\beta = 0.382$, and $\gamma = 1.7$ are empirical coefficients (see [12,13] for details); $d_{50} = 50\,\mu\mathrm{m}$ is the median sediment grain size; U is the magnitude of the local depth-averaged velocity; $B_i(\mathbf{x}, t)$ is the annually-averaged biomass production of vegetation species "i" which happens to colonize site $\mathbf{x}$ at time t (above-ground biomass, responsible for suspended sediment trapping, and below-ground biomass, responsible for organic soil production, are here assumed to be both equal to $B_i(\mathbf{x}, t)$; and $Q_{o_0} = 2.5 \times 10^{-6}\ \mathrm{m^3/yr/g}$ is a constant which incorporates typical vegetation characteristics and the density (after compaction and partial decomposition) of the organic soil produced.

The local annually-averaged biomass production, $B_i\ [z(\mathbf{x}, t)] = B_{\max}\ f_i\ [z(\mathbf{x}, t)]$, is expressed as a fraction of a maximum attainable value, $B_{\max} = 10^3\ \mathrm{g\,m^{-2}}$, through a species-specific fitness function, $0 < f_i(z) < 1$. The fitness function defines how biomass production and competitive abilities of each species vary with soil elevation, and hence describes the degree of adaptation of a species i to the local elevation z and to the related edaphic conditions (see [8,32] for further details).

Following Marani et al. [32] we adopt the following analytical relationship for the fitness function $f_i(z)$:

$$f_i = \frac{2}{e^{\lambda(\zeta - \hat{\zeta}_i)} + e^{\lambda(\zeta - \hat{\zeta}_i)}}, \tag{7}$$

where $\zeta = z/H$, $\hat{\zeta}_i = \hat{z}_i/H$ corresponds to the dimensionless elevation at which the fitness function for species i reaches its maximum value ($f(\hat{\zeta}_i) = 1$), and λ is a scale parameter, expressing the rate at

Please cite this article as: A. D'Alpaos, M. Marani, Reading the signatures of biologic–geomorphic feedbacks in salt-marsh landscapes, Advances in Water Resources (2015), http://dx.doi.org/10.1016/j.advwatres.2015.09.004

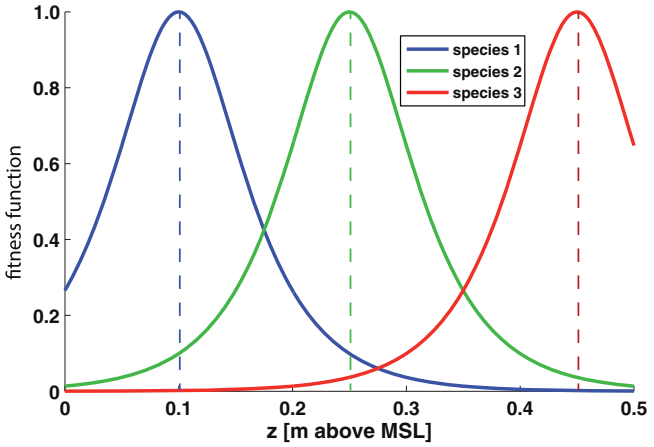

Fig. 2. Fitness functions for three vegetation species with the same degree of specialization ($\lambda = 10$, see Eq. (7)), characterized by different optimal elevations $\hat{z_1} = 0.10$ m, $\hat{z_2} = 0.25$ m, and $\hat{z_3} = 0.45$ m above MSL for the "blue", "green", and "red" species, respectively. (For interpretation of the references to color in this figure legend, the reader is referred to the web version of this article.)

which the fitness function tends to zero (for $z \to \pm\infty$) as elevation deviates from the species-specific optimal value (Fig. 2). Eq. (7) accounts for the observation that halophytic vegetation species are maximally productive within specific ranges of optimal adaptation [47,48,57]. A large value of λ mimics the behavior of a specialized vegetation species, only fit within a narrow range of elevations. Conversely, a small value of λ characterizes species which are relatively well adapted to a broader range of marsh elevations.

Following Marani et al. [32] we assume that the fitness function not only describes biomass productivity, but also the species competitive abilities, which decrease as elevation deviates from the species-specific elevation value providing optimal environmental conditions. Competition is represented here through two possible modelling approaches. According to the "fittest-takes-all" mechanism [32] we assume that a vegetation species "j", which at time t colonizes a site $\mathbf{x}_k$ with elevation $z_k(\mathbf{x}, t)$, is replaced by another species "i" if $f_i(z_k) > f_j(z_k) \forall j \neq i$ (i.e. species i is best adapted to the current value of the elevation). This mechanism, which selects at each time step and at each site the species i for which f_i is largest, allows us to study system equilibria and patterns in the ideal case in which the outcome of vegetation dynamics can be isolated from the effects of stochasticity (in the environment and in the organisms). Marani et al. [32] also consider a "stochastic competition" mechanism, according to which vegetation distribution at each site $\mathbf{x}_k$ is updated at each time step by randomly selecting a species i with a probability $p_i(z_k) = f_i(z_k)/\sum_j f_j(z_k)$. Although this second criterion appears to more realistically account for real-life stochastic conditions, the first has the advantage of more clearly illustrating vegetation controls on marsh morphology.

Before describing how the system evolves in time, we note that marsh-surface elevations evolve over time scales of one to several years, and therefore Eq. (2) may be regarded as the annually-averaged mass balance equation. Conversely, sediment dynamics over the platform, governed by Eq. (1) is controlled by changes in the hydrodynamic flow field on subhourly time scales, and can therefore be solved separately. Hence, coupled biogeomorphological simulations proceed as follows. At a given morphological time step for which the distributions of soil elevations and vegetation species over the platform are known, the hydrodynamic field is determined and the advection–dispersion equation is solved throughout a tidal cycle. The local organic accretion rate, $Q_o(\mathbf{x}, t) = Q_{o_0}\, B_{\max}\, f_i(z(\mathbf{x}, t))$, "$i$" being the species currently occupying site $\mathbf{x}$ at time t, is computed. The local sedimentation, $Q_d(\mathbf{x}, t)$, and erosion, $Q_e(\mathbf{x}, t)$, fluxes are determined and integrated over a tidal cycle to obtain bottom elevation changes $(\partial z(\mathbf{x}, t)/\partial t)$. These are then multiplied by a morphological factor m_f to compute changes in marsh topography over a time-dependent number (m_f) of tidal cycles (see [12] for a detailed description), on the basis of an "off-line" procedure [62]. Subsequently, the species distribution is updated according to the new topographic configuration (using the "fittest-takes-all" or the stochastic competition mechanism), and a new morphological time step is started.

3. Results and discussion

We carried out several numerical experiments in a computational domain designed to reproduce the geometry of a tidal watershed within the San Felice salt marsh (northern Venice Lagoon, see inset in Fig. 1b and [35] for details on the study area). We assumed a forcing semidiurnal sinusoidal tide with amplitude of 0.50 m, oscillating around MSL.

We analyzed the influence of: (1) sediment supply, (2) rate of RSLR, and (3) vegetation biomass productivity and competitive abilities on salt-marsh biogeomorphic patterns. It is worth noting that, although our simulations were carried out within an actual tidal watershed in the Venice lagoon, model parameters were not calibrated with reference to any particular setting and the numerical experiments were not aimed at modelling a particular environment. Our objective is rather to analyze the marsh biogeomorphic equilibria emerging as a result of different environmental forcing and vegetation characteristics.

Before describing in detail the influence of environmental forcing and vegetation characteristics on salt-marsh features, it is worthwhile discussing the general biogeomorphological patterns resulting from the underlying feedbacks between water fluxes, sediment transport, and vegetation dynamics which emerge from the simulation of a reference case. We first consider a marsh platform forced with a SSC $C_0 = 10$ mg/l and a rate of RSLR $R = 5.0$ mm/yr, which can be populated by three vegetation species with the same degree of specialization ($\lambda = 10$), characterized by different optimal elevations $\hat{z_1} = 0.10$ m, $\hat{z_2} = 0.25$ m, and $\hat{z_3} = 0.45$ m above MSL for the "blue", "green", and "red" species, respectively, as depicted in Fig. 2. All species are characterized by equal maximum fitness and therefore by an equal maximum annually-averaged biomass production.

Fig. 3 a shows marsh surface elevations in equilibrium with the prescribed rate of RSLR and SS, and allows one to distinguish the sedimentation patterns which characterize the non-uniform marsh topography when the "fittest-takes-all" mechanism is considered. Marsh topography is characterized by the formation of higher levees paralleling channel banks and elevations which progressively decrease toward the inner portion of the marsh. The reduction in the SSC with distance from the channel network, as a consequence of inorganic deposition (due to settling and direct particle capture by plant stems) and the decrease in sediment transport capability of tidal flows, is responsible for the development of a typical concave-up profile at the marsh scale (e.g., [10,64,69] and Fig. 1 for a qualitative comparison). However, at a smaller scale one observes a marked transition between neighboring gently sloping terrace-like structures [8,32], that indeed result from the coupled evolution of topography and vegetation cover. Fig. 3b shows the spatial distribution of the different vegetation species corresponding to the marsh topographic patterns of Fig. 3a. The gently sloping areas colonized by a single vegetation species, displaying sharp transitions among them, are very much reminiscent of the zonation patterns observed across marshes worldwide [e.g., 1, [5,56,64,31], 44]. Model results also suggest that about 15% of marsh area is lost (black unchanneled portions of the platform in Fig. 3a), making the transition to a tidal flat [10,27,33,73]. Marsh loss due to "drowning" occurs at sites near the watershed divide, where the advective transport is reduced as well as the settling rate, and the marsh cannot keep pace with the imposed rate of RSLR [10]. The observation that marsh submergence does not occur

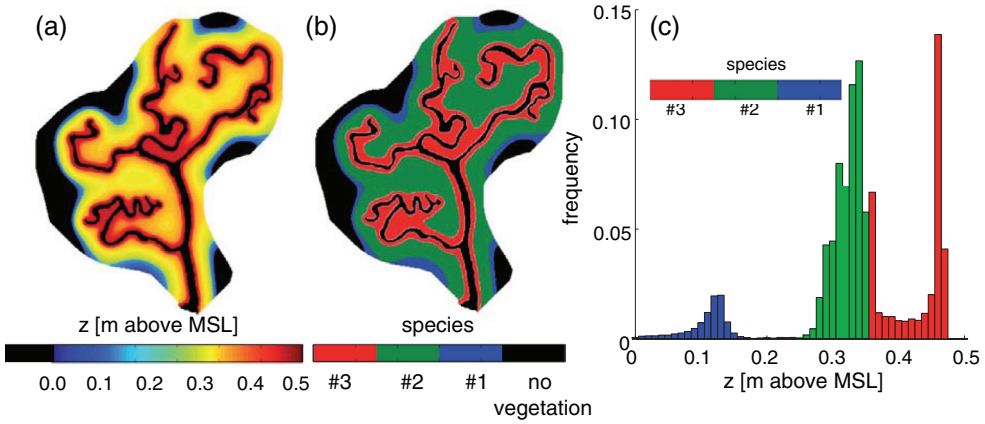

Fig. 3. Reference case ($C_0 = 10$ mg/l, $R = 5.0$ mm/yr, three vegetation species with $\lambda = 10$, see Fig. 2). (a) Color-coded representation of equilibrium topography for the reference case. Marsh surface elevations are referenced to MSL. (b) Color-coded representation of vegetation cover. (c) Multimodal frequency distribution of topographic elevations in which color codes represent the different species populating different elevation intervals. (For interpretation of the references to color in this figure legend, the reader is referred to the web version of this article.)

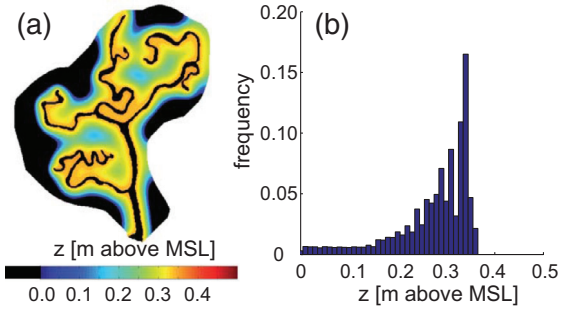

Fig. 4. Unvegetated case ($C_0 = 10$ mg/l, $R = 5.0$ mm/yr, as in the reference case of Fig. 3, without vegetation). (a) Color-coded representation of equilibrium topography, where marsh surface elevations are referenced to MSL. (b) Frequency distribution of topographic elevations. (For interpretation of the references to color in this figure legend, the reader is referred to the web version of this article.)

catastrophically, but rather, preferentially starting with inner portions of the marsh supports similar conclusions drawn in a 1D context by Da Lio et al. [8] and Ratliff et al. [59] and also agrees with field observations [17,20]. The surviving marsh is characterized by an average elevation $z_{mean} = 0.34$ m above MSL, whereas the average marsh elevations of the "blue", "green", and "red" patches is equal to 0.11 m, 0.32 m, and 0.43 m, respectively.

Fig. 3 c shows the frequency distribution of topographic marsh elevations and highlights the crucial role of bio-geomorphic feedbacks in determining the observed coupled topographic and vegetation patterns. The frequency distribution of marsh elevations displays a multimodal behavior, each frequency maximum being robustly associated with a single vegetation species. The close relationship between peaks in the frequency distribution and vegetation species is found to be a characteristic signature of the underlying and intertwined physical and biological processes in marsh landscapes. This correspondence between species presence and the peaks in the frequency distribution of elevations constitutes a detectable fingerprint of the landscape-constructing role of marsh plants [32].

The crucial role of biologic–geomorphic feedbacks in producing characteristic landscape features emerges most clearly when considering the equilibrium topography, and the corresponding frequency distribution of topographic elevations, in the hypothetical situation in which vegetation is absent (Fig. 4: $C_0 = 10$ mg/l and $R = 5.0$ mm/yr). The frequency distribution of topographic elevations displays a single mode, dictated by the preferential deposition of suspended sediments near the creeks. The characteristic signature of two-way bio-geomorphic interactions (i.e., multiple peaks in the frequency distribution associated to different vegetation species) is absent in this case. Moreover, with respect to the vegetated case, larger salt marsh areas are lost due to "drowning". About 30% of the area is below MSL in the nonvegetated case (black unchanneled portions of the platform in Fig. 4a), and has made the transition to a tidal flat. This enhanced drowning occurs because, without vegetation, trapping and organic production are additionally absent. We conclude that sites near the watershed divide, where only modest quantities of suspended sediment are advected, crucially rely organic soil production to keep up with RSLR. The surviving marsh is characterized by an average elevation $z_{mean} = 0.27$ m above MSL (to be compared to the average marsh elevation in the reference case was $z_{mean} = 0.34$ m above MSL). The increased presence of drowned areas in the nonvegetated case highlights the importance of salt-marsh vegetation in maintaining elevations above MSL.

The spatially-extended impacts of changes in the rates of RSLR and SS can also be studied. Changes in the rate of RLSR have more spatially-extensive effects on marsh elevation (Fig. 5) and species distribution (Fig. 6). A decrease in the rate of RSLR from 5 mm/yr to 3 mm/yr (a 40% decrease) causes the whole domain to reach a vegetated equilibrium located above MSL (compare the second row of topographies with the third row of topographies in Fig. 5). An increase in sediment supply from 20 mg/l to 30 mg/l (a 50% increase) barely affects the fraction of the domain located above MSL (compare the second and the third column in Fig. 5) and mostly increases marsh elevation in areas closer to the creeks. Our numerical observations, although based on limited variations in the considered environmental forcings (rates of RSLR in the range 3 – 7 mm/yr and SSC in the range 10 – 30 mg/l), suggest that changes in SS might not be able to balance or partially offset the impacts of RSLR because the spatial patterns produced differ significantly. Increasing SS to microtidal coastal marshes (e.g. from 10 to 30 mg/l) might not be able to compensate for rising sea levels (e.g. from 3 to 5–7 mm/yr) because of the spatially explicit dynamics. However, we deem worth emphasizing that although increasing rates of RSLR have a strong effect on marsh survival possibly leading to marsh drowning, decreasing SS are likely to produce a similar result, thus leading to marsh collapse.

The lowest-lying species (blue species in Fig. 6) tends to be most sensitive to changes in the rate of RSLR. When R is increased from 3 mm/yr to 5 mm/yr, the lowest-lying species is favored because it can contribute to stabilize some areas at equilibrium elevations within its range of optimality (compare second and third rows in Fig. 6). A further increase in R (see the first row in Fig. 6) instead has the effect of reducing the extent of the area colonized by the "lowest"

Please cite this article as: A. D'Alpaos, M. Marani, Reading the signatures of biologic–geomorphic feedbacks in salt-marsh landscapes, Advances in Water Resources (2015), http://dx.doi.org/10.1016/j.advwatres.2015.09.004

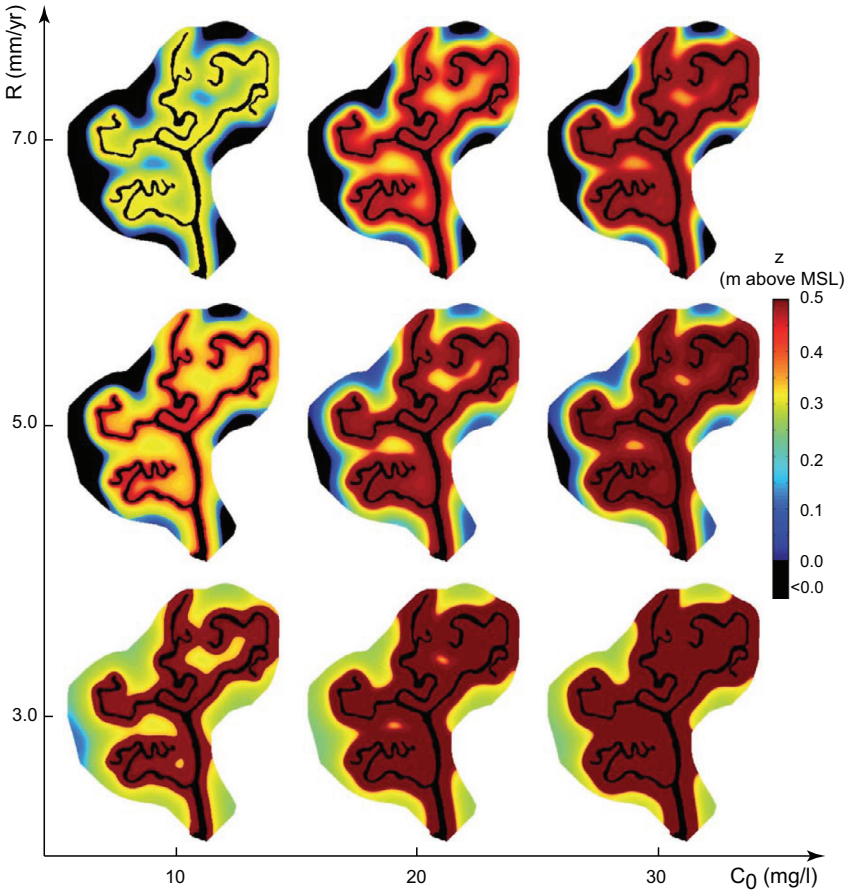

Fig. 5. Color-coded representation of marsh surface elevations (referenced to MSL) in equilibrium with different rates of relative SLR (in the range 3 – 7 mm/yr) and different values of the SSC within the channel network (in the range 10 – 30 mg/l), when the marsh is forced by a semidiurnal tide of amplitude 0.5 m and populated by three different vegetation species with fitness functions shown in Fig. 2. The "fittest-takes-all" mechanism is considered in this case. (For interpretation of the references to color in this figure legend, the reader is referred to the web version of this article.)

blue species, which is squeezed between expanding tidal flats (black areas below MSL) and areas colonized by higher-lying species. On the contrary, the lowest lying species is fairly insensitive to changes in SS (compare the second and the third column in Fig. 5), as relatively little suspended sediment is advected far from the creeks and makes it to the inner parts of the marsh. The species colonizing the higher elevation ranges are mostly affected by SS, and only secondarily by the rate of RSLR. For large sediment supplies (second and third columns in Fig. 6) the extent of the areas colonized by the red and the green species is not very sensitive to changes in the rate of RSLR. Only for low sediment supply levels (first column in Fig. 6) is the "highest" (red) species sensitive to changes in RSLR, disappearing for $R = 7$ mm/yr. Overall, the "intermediate" (green) species seems to be most resilient to current environmental trends, characterized by decreasing sediment delivery to the coastal zone [65], and by increased rates of RSLR. Model results suggest that marsh elevations decrease with increasing rates of RSLR and decreasing SS (e.g., [33,25,11]) and marsh loss due to drowning increases with increasing rates of RSLR and decreasing SS (e.g., [27,10]). More interestingly, our analyses also emphasize that biodiversity is influenced by the environmental forcings (rate of RSLR and SS in this case): changes in the rate of RSLR and/or in SS may, in fact, result in the selective disappearance of some or all of the stable equilibria associated with marsh biologic–geomorphic patterns, with consequent reductions in the biodiversity.

Fig. 7 shows the results of model simulations aimed at analyzing the effects of vegetation characteristics (namely, vegetation specialization and biodiversity) and of environmental heterogeneities (through the selection mechanism) on intertwined physical and biological processes, on the emerging bio-geomorphic patterns, and their signatures possibly imprinted in the salt-marsh landscape. When the marsh is encroached by less specialized vegetation species ($\lambda = 5$, Fig. 7a1–d1) than in the reference case ($\lambda = 10$), the resulting topographies display smoother transitions between patches (Fig. 7b1) thus suggesting a milder vegetation control on marsh biomorphodynamic processes [8]. Such a behavior is also confirmed by the frequency distribution of marsh elevations (Fig. 7d1) which still displays a multimodal behavior, although characterized by less-pronounced peaks. The effects of two-way bio-geomorphic feedbacks are still fingerprinted in the landscape and their characteristic signatures can still be identified. In addition, model results show that the average marsh elevation slightly increases ($z_{mean} = 0.37$m above MSL compared to $z_{mean} = 0.34$ m in the reference case), the average elevations of the three patches remain almost unchanged, whereas the variability of within-patch elevations slightly increases (Fig. 7 b1 and d1) together with within-patch topographic gradients. About 15% of marsh area is lost due to "drowning", as in the reference case (Fig. 3). The extent of the area colonized by the different vegetation species (Fig. 7c1) does not change for "lowest" blue species (about 12% in the less-specialized compared to about 9% in the reference case), increases for the "higher-lying" red species (from 34% to 62%), and decreases for the "intermediate" green species (from 57% to 26%).

When more-specialized vegetation species ($\lambda = 15$, Fig. 7a2–d2) are considered, marsh topographies (Fig. 7b2) and the resulting bio-geomorphic patterns are more "focused" within narrow elevation ranges (Fig. 7c2 and d2). Compared to the reference case, the average marsh elevation slightly decreases ($z_{mean} = 0.31$ m), the

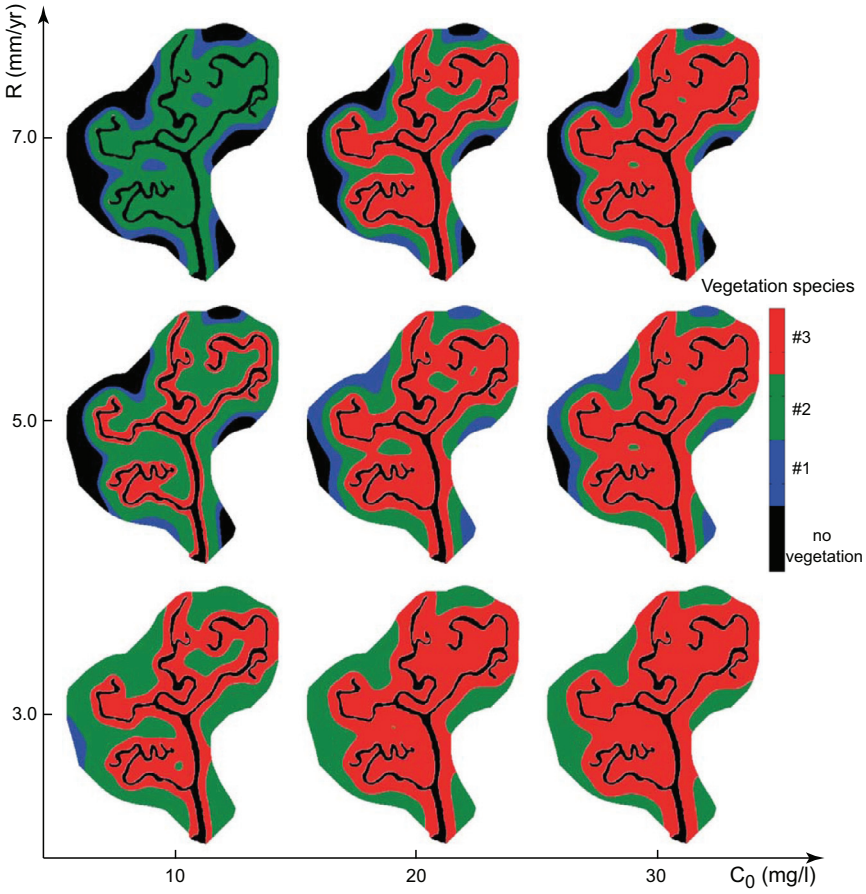

Fig. 6. Color-coded representation of vegetation patterns in equilibrium with topographic elevations of Fig. 4, when the marsh is forced by different rates of relative SLR (in the range 3 – 7 mm/yr) and different values of the SSC within the channel network (in the range 10 – 30 mg/l). The "fittest-takes-all" mechanism is considered in this case. (For interpretation of the references to color in this figure legend, the reader is referred to the web version of this article.)

average elevations of the "lowest" (blue) and "intermediate" (green) patches remain almost unchanged, whereas the average elevation of the "higher" (red) patch decreases (from $z_{mean} = 0.43$ m above MSL in the reference case to $z_{mean} = 0.37$). The variability of within-patch elevations decreases (Fig. 7b2 and d2) together with within-patch topographic gradients. About 15% of marsh area drowns, as in the reference case. The extent of the area colonized by the "lowest" blue species remains almost unchanged (about 8% while it was about 9% in the reference case), whereas an increase is observed for the 'intermediate" green species (from 57% to 73%) and a decrease is observed for the "higher-lying" red species (from 34% to 19%).

The effects of environmental stochasticity (e.g., heterogeneities in edaphic conditions or stochasticity in competition mechanisms) can be mimicked by considering the "stochastic competition" mechanism considered by Marani et al. [32] and Da Lio et al. [8]. Fig. 7a3–d3 and a4–d4 portrays the case in which the "stochastic competition" rule is adopted for vegetation species with $\lambda = 10$ (as in the reference case) and $\lambda = 5$, respectively. In both cases the major difference with the corresponding cases in which the "fittest takes all" rule was used (Figs. 3 and 7 a1–d1, respectively) consists in the emergence of relatively noisy and more realistic bio-geomorphic patterns, in which patches of mixed vegetation species replace vegetation patches previously populated by single species. Interestingly, one can still detect the multimodal frequency distribution of topographic elevations, the fingerprint of the underlying biogeomorphic feedbacks responsible for forming the observed zonation patterns. The frequency density of marsh elevations displays frequency maxima which are strongly associated with one vegetation species (as shown by color-coded bars according to the most abundant species colonizing each elevation interval) as clearly shown by observed frequency distributions in the Venice Lagoon [8,32]. The percentage of marsh areas which drown increases to about 23% and 21% for the cases with $\lambda = 10$ and $\lambda = 5$, respectively. This enhanced drowning occurs because the "lowest" (blue) species, characterized by larger biomass productivity at lower elevations, which deterministically encroached low-lying marsh portions in the "fittest takes all" case, is now replaced by the other two species. These species are less productive at lower elevations and therefore their trapping and organic production contributions to accretion are negligible.

We finally address the possible role of vegetation biodiversity and consider the case of a monospecific vegetation scenario in which the marsh can only be populated by the 'intermediate" green species (Fig. 7a5–d5). The average marsh elevation remains unchanged compared to the reference case, whereas the percentage of drowned marsh areas increases to about 21% due to the small biomass productivity of the green species at lower elevations, and the related lack of trapping and organic production. More interestingly, the frequency distribution of topographic elevations displays a single mode associated to the presence of the green species. Multiple peaks in the frequency distribution of topographic elevations are therefore observed only when different vegetation species compete each other to colonize the salt-marsh surface, and therefore represent the distinctive signature of the strong feedbacks between sediment transport and vegetation dynamics.

Silvestri et al. [64] analyzed several properties of the frequency distributions of halophytic vegetation species for four different marshes in the Venice Lagoon. Their analyses showed that an identical order of vegetation species, with respect to soil elevation, could

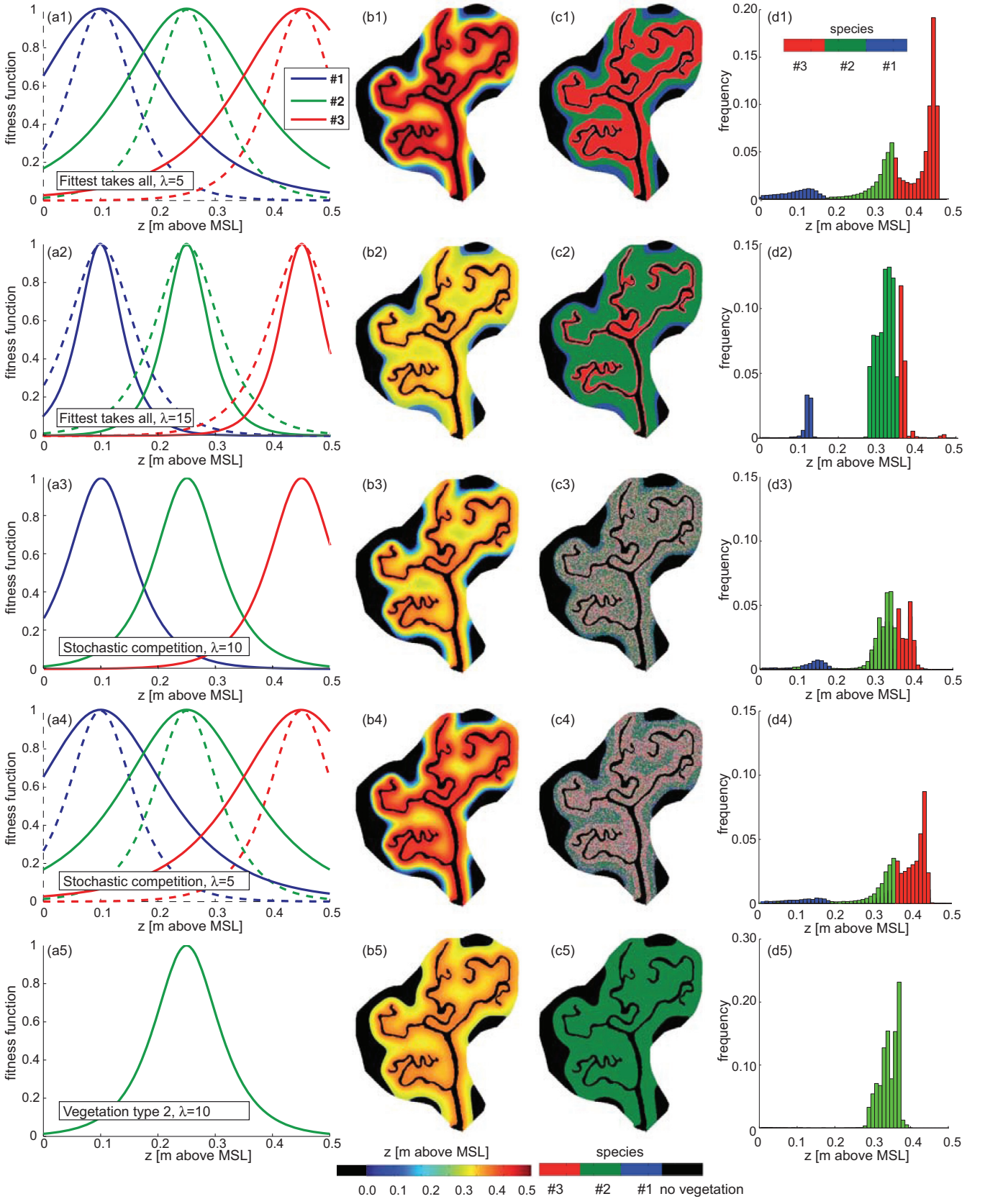

Fig. 7. Analysis of the role of vegetation specialization and of the competition mechanism, when the marsh is forced with a SSC $C_0 = 10$ mg/l and a rate of RSLR $R = 5.0$ mm/yr. (a1–a5) Different fitness functions considered in the analysis: (a1) $\lambda = 5$ ("less specialized species") and optimal elevations as in the reference case of Fig. 2; (a2) $\lambda = 5$ ("more specialized species") and optimal elevations as in Fig. 2; (a3) "Stochastic competition mechanisms" for vegetations with fitness functions as in the reference case of Fig. 2; (a4) "Stochastic competition mechanisms" for "less specialized species" $\lambda = 5$ and optimal elevations as in Fig. 2; (a5) "Monospecific scenario" with one vegetation species ("green species" of Fig. 2 ($\lambda = 5$). (b1–b5) Comparison of marsh equilibrium topography. (c1–c5) Comparison of vegetation cover. (d1–d5) Comparison of frequency distribution of elevations. (For interpretation of the references to color in this figure legend, the reader is referred to the web version of this article.)

Please cite this article as: A. D'Alpaos, M. Marani, Reading the signatures of biologic–geomorphic feedbacks in salt-marsh landscapes, Advances in Water Resources (2015), http://dx.doi.org/10.1016/j.advwatres.2015.09.004

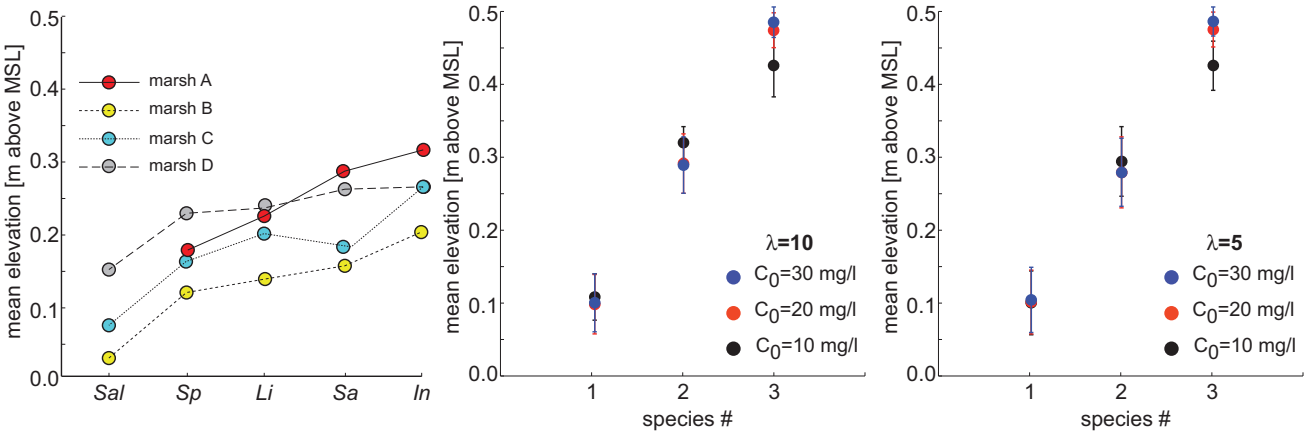

Fig. 8. (a) Mean marsh elevations for different vegetation species for four salt marshes (A–D) in the Venice lagoon observed by Silvestri et al. [64]. (b) Mean marsh elevations and standard deviations for the three considered vegetation species (in the reference case ($\lambda = 10$) of Fig. 2) as a function of different values of the forcing SSC (in the range $10 - 30$ mg/l) in the case of a rate of RSLR $R = 5.0$ mm/yr. (c) Same as in Fig. 8 in the case of 'less specialized species" with $\lambda = 5$.

be detected at the different marshes (Fig. 8a). Surprisingly, they also observed that the same species sequence was shifted vertically at different marshes and that a given species was best adapted to live at a preferential elevation, which differed in the different considered marshes. Here we tried to explain such shift in the sequence of marsh plants by considering marshes subjected to the same environmental forcings (tidal amplitude and period, rate of RSLR, watershed dimension and drainage density) apart from the forcing SSC (Fig. 8b and c). Our results show that the mean elevation characterizing a given vegetation species increases as the SS increases, and that the same sequence of vegetation species can be found at "different marshes" with different sediment supplies. Changes in the mean elevation of a single species with SS are more evident for the "higher" species and mildly depend on vegetation specialization (compare the cases of Fig. 8b and c, with $\lambda = 10$ and $\lambda = 5$, respectively). Similar results are found when considering different rates of RSLR, with changes in the mean elevation of a single species found to increase with the rate of RSLR. Model results might thus help explaining why the same species can be found to grow at different ranges of soil elevations over different marshes, while preserving the same species sequence which is shifted vertically. Nevertheless, it is worth noting multiple factors can play an important role in determining the observed and modelled distribution of halophytic plants. In particular, a combination of spatial heterogeneities of soil properties together with evapotranspiration patterns and subsurface water dynamics, which control root oxygen availability, are likely to exert a fundamental control on vegetation patterns [36,43,64,76].

4. Conclusions

We have provided a two-dimensional representation of salt-marsh biomorphodynamics which allows us to highlight the crucial role of interacting physical and biological processes and detect their signatures possibly imprinted in the salt-marsh landscape. Biogeomorphic feedbacks critically affect the response and the resilience of salt-marsh landscapes to changes in the environmental forcing.

The development and application of the fully two-dimensional model of marsh bio-geomorphology also highlight how marsh responses to changes in forcings are highly spatially dependent. Changes in sediment supply most directly and deeply affect marsh areas closest to the tidal network. These areas mostly accrete through inorganic sediment deposition, and thus more readily respond to variations in the suspended sediment concentration. Changes in the rate of RSLR affect the marsh platform as a whole, but submergence occurs first in the inner parts of the marsh, located further away from the tidal creek. This observation extends similar conclusions drawn in a 1D context by Da Lio et al. [8] and Ratliff et al. [59] and implies that marsh conversion into tidal flats, which may be caused by increased rates of RSLR or decreasing SS, does not occur catastrophically, as a zero-dimensional stability analysis would suggest, but rather through a progressive, if rapid, retreat of the marsh area.

The growth and presence of halophytic vegetation on salt-marsh surfaces increases the vertical accretion rates, thus enhancing the resilience of marshes to increasing rates of RSLR. Marsh portions near watershed divides crucially rely on organic soil production to keep up with RSLR and therefore physical–biological feedbacks are crucial for salt-marsh presence and continued existence.

Not only biodiversity is influenced by the environmental forcings (rate of RSLR and SS in the cases considered here), but also a lower species diversity influences the response of salt-marsh landscapes to changes in the forcings. If one the one hand, changes in the rate of RSLR and/or in SS may result in a reduction in biodiversity through the disappearance of some or all of the stable equilibria associated with marsh bio-geomorphic patterns, on the other hand lower species diversity of plants decreases marsh ability to face increasing rates of RSLR.

The spatially extended model presented also allows us to generate realistic frequency distributions of vegetation occurrence. Multimodal frequency distributions of marsh elevations, known to be the fingerprint of the landscape-constructing role of marsh plants, emphasize how vegetation species shape the marsh landscape (to various degrees depending on the range of marsh elevations to which they are adapted) leading to the formation of bio-geomorphic zonation patterns. These landscape features would not have emerged in the absence of interactions and feedbacks between sediment transport and multiple-species vegetation dynamics.

We suggest that these distributions can now be used as hypotheses to be tested through field or remote sensing characterization of vegetation distribution. Furthermore, because such distributions are linked to the physiological responses of vegetation to edaphic conditions, they can be used to investigate the "fitness functions", or species responses to the controlling stressor (surrogated by elevation in the present case).

Experimenting with different sediment supply levels, a near impossibility in real field conditions, allowed us to identify the effects of such differences on ecogeomorphic observables. In particular, although multiple factors can play an important role in determining the distribution of halophytes, the model suggests that the same species can be found at different elevations in different marshes, forced with different sediment supplies, while preserving the "order", with

Please cite this article as: A. D'Alpaos, M. Marani, Reading the signatures of biologic–geomorphic feedbacks in salt-marsh landscapes, Advances in Water Resources (2015), http://dx.doi.org/10.1016/j.advwatres.2015.09.004

respect to elevation, in which the different competing species can be found.

Acknowledgments

This work was supported by the CARIPARO Project titled "Reading signatures of the past to predict the future: 1000 years of stratigraphic record as a key for the future of the Venice Lagoon", that is gratefully acknowledged.

References

[1] Adam P. Salt-marsh ecology. Cambridge,UK: Cambridge University Press; 1990.
[2] Allen J. Salt-marsh growth and stratification: a numerical model with special reference to the Severn Estuary, southwest Britain. MarGeol 1990;95(2):77–96.
[3] Belliard J, Toffolon M, Carniello L, D'Alpaos A. An ecogeomorphic model of tidal channel initiation and elaboration in progressive marsh accretional context. Geophys Res Lett 2015;120:1040–64. http://dx.doi.org/10.1002/2015JF003445.
[4] Boaga J, D'Alpaos A, Cassiani G, Marani M, Putti M. Plant-soil interactions in salt marsh environments: experimental evidence from electrical resistivity tomography in the Venice Lagoon. Geophys Res Lett 2014;41:6160–6. http://dx.doi.org/10.1002/2014GL060983.
[5] Chapman V. Coastal vegetation. 2nd ed. Pergamon Press, Oxford; 1976.
[6] Chmura G, Anisfeld S, Cahoon D, Lynch J. Global carbon sequestration in tidal, saline wetland soils. GlobalBiogeochem Cycles 2003;17(4):12 pages. http://dx.doi.org/10.1029/2002GB001917.
[7] Costanza R, d'Arge R, de Groot R, Farberk S, Grasso M, Hannon B, et al. The value of the world's ecosystem services and natural capital. Nature 1997;387:253–60.
[8] Da Lio C, D'Alpaos A, Marani M. Vegetation engineers marsh morphology through competing multiple stable states. Philos Trans R Soc A 2013;371:20120367. http://dx.doi.org/10.1098/rsta.2012.0367.
[9] Dacey JWH, Howes BL. Water uptake by roots controls water table movement and sediment oxidation in short *Spartina* marsh. Science 1984;224:487–9. http://dx.doi.org/10.1126/science.224.4648.487.
[10] D'Alpaos A. The mutual influence of biotic and abiotic components on the long-term ecomorphodynamic evolution of salt-marsh ecosystems. Geomorphology 2011;126:269–78. http://dx.doi.org/10.1016/j.geomorph.2010.04.027.
[11] D'Alpaos A, Da Lio C, Marani M. Biogeomorphology of tidal landforms: physical and biological processes shaping the tidal landscape. Ecohydrology 2012;5:550–62. http://dx.doi.org/10.1002/eco.279.
[12] D'Alpaos A, Lanzoni S, Marani M, Rinaldo A. Landscape evolution in tidal embayments: modeling the interplay of erosion sedimentation and vegetation dynamics. J Geophys Res 2007;112:F01008. http://dx.doi.org/10.1029/2006JF000537.
[13] D'Alpaos A, Lanzoni S, Mudd S, Fagherazzi S. Modelling the influence of hydroperiod and vegetation on the cross-sectional formation of tidal channels. Estuarine Coastal Shelf Sci 2006;69:311–24. http://dx.doi.org/10.1016/j.ecss.2006.05.002.
[14] D'Alpaos A, Mudd S, Carniello L. Dynamic response of marshes to perturbations in suspended sediment concentrations and rates of relative sea level rise. J Geophys Res 2011;116:F04020. http://dx.doi.org/10.1029/2011JF002093.
[15] D'Alpaos L, Defina A. Mathematical modeling of tidal hydrodynamics in shallow lagoons: a review of open issues and applications to the Venice Lagoon. Comput Geosci 2007;33(4):476–96. http://dx.doi.org/10.1016/j.cageo.2006.07.009.
[16] Day J, Shaffer G, Britsch L, Reed D, Hawes S, Cahoon D. Pattern and process of land loss in the Mississippi Delta: a spatial and temporal analysis of wetland habitat change. Estuaries 2000;23:425–38. http://dx.doi.org/10.2307/1353136.
[17] DeLaune R, Nyman J, Patrick JW. Peat collapse, ponding and wetland loss in a rapidly submerging coastal marsh. J Coastal Res 1994;10(4):1021–30.
[18] Dietrich WE, Perron JT. The search for a topographic signature of life. Nature 2006;439:411–18. http://dx.doi.org/10.1038/nature04452.
[19] Einstein H, Krone R. Experiments to determine modes of cohesive sediment transport in salt water. J Geophys Res 1962;67(4):1451–61.
[20] Erwin R, Sanders G, Prosser D. Changes in lagoonal marsh morphology at selected northeastern Atlantic coast sites of significance to migratory waterbirds. Wetlands 2004;24(4):891–903. http://dx.doi.org/10.1672/0277-5212(2004)024[0891:CILMMA]2.0.CO;2.
[21] Fagherazzi S, Kirwan L, Mudd S, Guntenspergen G, Temmerman S, D'Alpaos A, et al. Numerical models of salt marsh evolution: ecological, geomorphic, and climatic factors. Rev Geophys 2012;50:RG1002. http://dx.doi.org/10.1029/2011RG000359.
[22] Fourqurean J, Duarte C, Kennedy H, Marba N, Holmer M, Mateo MA, et al. Seagrass ecosystems as a globally significant carbon stock. Nat Geosci 2012;5:505–9. http://dx.doi.org/10.1038/NGEO1477.
[23] Gedan KB, Kirwan M, Wolanski E, Barbier E, Silliman B. The present and future role of coastal wetland vegetation in protecting shorelines: answering recent challenges to the paradigm. Clim Change 2011;106:7–29. http://dx.doi.org/10.1007/s10584-010-0003-7.
[24] Howes NC. Hurricane-induced failure of low salinity wetlands. Proc Natl Acad Sci USA 2010;107(32):14014–19. http://dx.doi.org/10.1073/pnas.0914582107.
[25] Kirwan M, Guntenspergen G, D'Alpaos A, Morris J, Mudd S, Temmerman S. Limits on the adaptability of coastal marshes to rising sea level. Geophys Res Lett 2010;37:L23401. http://dx.doi.org/10.1029/2010GL045489.
[26] Kirwan M, Mudd S. Response of salt-marsh carbon accumulation to climate change. Nature 2012;489:550–3. http://dx.doi.org/10.1038/nature11440.
[27] Kirwan M, Murray A. A coupled geomorphic and ecological model of tidal marsh evolution. Proc Natl Acad Sci USA 2007;104(15):6118–22. http://dx.doi.org/10.1073/pnas.0700958104.
[28] Larsen LG, Harvey JW. How vegetation and sediment transport feedbacks drive landscape change in the Everglades and wetlands worldwide. Am Natur 2010;176:E66–79. http://dx.doi.org/10.1086/655215.
[29] Larsen LG, Moseman S, Santoro AE, Hopfensperger K, Burgin A. A complex systems approach to predicting effects of sea level rise and nitrogen loading on nitrogen cycling in coastal wetland ecosystems. In: Kemp PF, editor. Eco-DAS VIII symposium proceedings. Waco, TX: Association for the Sciences of Limnology and Oceanography; 2010. http://dx.doi.org/10.4319/ecodas.2010.978-0-9845591-1-4.67.
[30] Leonard LA, Luther ME. Flow hydrodynamics in tidal marsh canopies. Limnol Oceanogr 1995;40(8):1474–84.
[31] Marani M, Belluco E, Ferrari S, Silvestri S, D'Alpaos A, Lanzoni S, et al. Analysis, synthesis and modelling of high-resolution observations of salt-marsh eco-geomorphological patterns in the Venice Lagoon. Estuarine Coastal Shelf Sci 2006;69(3–4):414–26. http://dx.doi.org/10.1016/j.ecss.2006.05.021.
[32] Marani M, Da Lio C, D'Alpaos A. Vegetation engineers marsh morphology through competing multiple stable states. Proc Natl Acad Sci USA 2013;110:3259–63. http://dx.doi.org/10.1073/pnas.1218327110.
[33] Marani M, D'Alpaos A, Lanzoni S, Carniello L, Rinaldo A. Biologically controlled multiple equilibria of tidal landforms and the fate of the Venice Lagoon. Geophys Res Lett 2007;34:L11402. http://dx.doi.org/10.1029/2007GL030178.
[34] Marani M, D'Alpaos A, Lanzoni S, Carniello L, Rinaldo A. The importance of being coupled: Stable states and catastrophic shifts in tidal biomorphodynamics. J Geophys Res 2010;115:F04004. http://dx.doi.org/10.1029/2009JF001600.
[35] Marani M, Lanzoni S, Belluco E, D'Alpaos A, Defina A, Rinaldo A. On the drainage density of tidal networks. Water Resour Res 2003;39(2):105–13. http://dx.doi.org/10.1029/2001WR001051.
[36] Marani M, Silvestri S, Belluco E, Ursino N, Comerlati A, Tosatto O, et al. Spatial organization and ecohydrological interactions in oxygen-limited vegetation ecosystems. Water Resour Res 2006;42:W07S06. http://dx.doi.org/10.1029/2005WR004582.
[37] Marani M, Zillio T, Belluco E, Silvestri S, Maritan A. Non-neutral vegetation dynamics. PLoS ONE 2006;1(1):5 pages. http://dx.doi.org/10.1371/journal.pone.0000078.
[38] Mariotti G, Carr J. Dual role of salt marsh retreat: long-term loss and short-term resilience. Water Resour Res 2014;50:2963–74. http://dx.doi.org/10.1002/2013WR014676.
[39] Mariotti G, Fagherazzi S. A numerical model for the coupled long-term evolution of salt marshes and tidal flats. J Geophys Res 2010;115:F01004. http://dx.doi.org/10.1029/2009JF001326.
[40] Mcleod E, Chmura G, Bouillon S, Salm R, Bjork R, Duarte C, et al. A blueprint for blue carbon: toward an improved understanding of the role of vegetated coastal habitats in sequestering CO_2. Front Ecol Environ 2011;9:552–60. http://dx.doi.org/10.1890/110004.
[41] Mehta A. Characterization of cohesive sediment properties and transport processes in estuaries. In: Mehta AJ, editor. Estuarine cohesive sediment dynamics, Lecture notes on coastal and estuarine studies, vol. 14. Berlin: Springer-Verlag; 1984.
[42] Mitsch W, Gosselink J. Wetlands. Hoboken, NJ: John Wiley; 2000.
[43] Moffett KB, Gorelick SM, McLaren RG, Sudicky EA. Salt marsh ecohydrological zonation due to heterogeneous vegetation groundwater surface water interactions. Water Resour Res 2012;48:W02516. http://dx.doi.org/10.1029/2011WR010874.
[44] Moffett KB, Robinson DA, Gorelick SM. Relationship of salt marsh vegetation zonation to spatial patterns in soil moisture, salinity and topography. Ecosystems 2010;13:1287–302.
[45] Möller I, Kudella M, Rupprecht F, Spencer T, Maike P, van Wesenbeeck B, et al. Wave attenuation over coastal salt marshes under storm surge conditions. Nat Geosci 2014;7:727–31. http://dx.doi.org/10.1038/NGEO2251.
[46] Möller I, Spencer T, French J, Leggett D, Dixon M. Wave transformation over salt marshes: a field and numerical modelling study from North Norfolk, England. Estuarine Coastal Shelf Sci 1997;49:411–26. http://dx.doi.org/10.1006/ecss.1999.0509.
[47] Morris J. Competition among marsh macrophytes by means of geomorphological displacement in the intertidal zone. Estuarine Coastal Shelf Sci 2006;69:395–402. http://dx.doi.org/10.1016/j.ecss.2006.05.025.
[48] Morris J, Sundareshwar P, Nietch C, Kjerfve B, Cahoon D. Responses of coastal wetlands to rising sea level. Ecology 2002;83:2869–77. http://dx.doi.org/10.1890/0012-9658(2002)083[2869:ROCWTR]2.0.CO;2.
[49] Mudd S. The life and death of salt marshes in response to anthropogenic disturbance of sediment supply. Geology 2011;39(5):511–12. http://dx.doi.org/10.1130/focus052011.1.
[50] Mudd S, D'Alpaos A, Morris J. How does vegetation affect sedimentation on tidal marshes? Investigating particle capture and hydrodynamic controls on biologically mediated sedimentation. J Geophys Res 2010;115:F03029. http://dx.doi.org/10.1029/2009JF001566.
[51] Mudd S, Fagherazzi S, Morris J, DJ F. Flow, sedimentation, and biomass production on a vegetated salt marsh in South Carolina: toward a predictive model of marsh morphologic and ecologic evolution. In: Fagherazzi S, Marani M, Blum LK, editors. The ecogeomorphology of tidal marshes, coastal and estuarine studies, vol. 59. Washigton, D.C.: AGU; 2004.

[52] Mudd S, Howell S, Morris J. Impact of dynamic feedbacks between sedimentation, sea-level rise, and biomass production on near surface marsh stratigraphy and carbon accumulation. Estuarine, Coastal Shelf Sci 2009;82(3):377–89. http://dx.doi.org/10.1016/j.ecss.2009.01.028.
[53] Murray A, Knaapen M, Tal M, Kirwan M. Biomorphodynamics: physical-biological feedbacks that shape landscapes. Water Resour Res 2008;44:W11301. http://dx.doi.org/10.1029/2007WR006410.
[54] Neubauer S. Novel mechanism of stream formation in coastal wetlands by crab–fish–groundwater interaction. Estuarine Coastal Shelf Sci 2008;78(1). http://dx.doi.org/10.1016/j.ecss.2007.11.011.
[55] Nyman JA, Walters RJ, Delaune RD, Patrick WH. Marsh vertical accretion via vegetative growth. Estuarine Coastal Shelf Sci 2006;69. http://dx.doi.org/10.1016/j.ecss.2006.05.041.
[56] Pennings S, Callaway R. Salt marsh plant zonation: the relative importance of competition and physical factors. Ecology 1992;73:681–90. http://dx.doi.org/10.2307/1940774.
[57] Pennings S, Grant M, Bertness M. Plant zonation in low-latitudes salt marshes: disentangling the roles of flooding, salinity and competition. J Ecol 2005;93:159–67. http://dx.doi.org/10.1111/j.1365-2745.2004.00959.x.
[58] Perillo G, Wolanski E, Cahoon D, Brinson M. Coastal wetlands: an integrated ecosystem approach. Elsevier; 2009.
[59] Ratliff K, Braswell A, Marani M. Spatial response of coastal marshes to increased atmospheric CO_2, Proc Natl Acad Sci USA, http://dx.doi.org/10.1073/pnas.1516286112.
[60] Reinhardt L, Jerolmack D, Cardinale B, Vanacker V, Wright J. Dynamic interactions of life and its landscape: feedbacks at the interface of geomorphology and ecology,
[61] Rinaldo A, Fagherazzi S, Lanzoni S, Marani M, Dietrich WE. Tidal networks 2. Watershed delineation and comparative network morphology. Water Resour Res 1999;35(12):3905–17.
[62] Roelvink J. Coastal morphodynamic evolution techniques. Coastal Eng 2006;53(2):277–87. http://dx.doi.org/10.1016/j.coastaleng.2005.10.015.
[63] Saco P, Rodriguez J. Modeling ecogeomorphic systems. In: Shroder J, Baas ACW, editors. Treatise on geomorphology, vol. 2. San Diego, CA: Academic Press; 2013. http://dx.doi.org/10.1016/B978-0-12-374739-6.00038-5.
[64] Silvestri S, Defina A, Marani M. Tidal regime, salinity and salt-marsh plant zonation. Estuarine Coastal Shelf Sci 2005;62:119–30. http://dx.doi.org/10.1016/j.ecss.2004.08.010.
[65] Syvitski JP, Vrsmarty CJ, Kettner AJ, Green P. Impact of humans on the flux of terrestrial sediment to the global coastal ocean. Science 2005;308:376–80. http://dx.doi.org/10.1126/science.1109454.
[66] Tambroni N, Seminara G. A one-dimensional eco-geomorphic model of marsh response to sea level rise: wind effects, dynamics of the marsh border and equilibrium. J Geophys Res 2012;117:F03026. 25 pages. http://dx.doi.org/10.1029/2012JF002363.
[67] Temmerman S, Bouma T, Van de Koppel J, Van der Wal D, De Vries MB, Herman P. Impact of vegetation on flow routing and sedimentation patterns: three-dimensional modeling for a tidal marsh. J Geophys Res 2005;110:F04019. http://dx.doi.org/10.1029/2005JF000301.
[68] Temmerman S, Bouma TJ, Van de Koppel J, Van der Wal D, De Vries MB, Herman PMJ. Vegetation causes channel erosion in a tidal landscape. Geology 2007;35(7):631–4. http://dx.doi.org/10.1029/2004JF000243.
[69] Temmerman S, Govers G, Meire P, Wartel S. Simulating the long-term development of levee-basin topography on tidal marshes. Geomorphology 2004;63(1–2):39–55. http://dx.doi.org/10.1016/j.geomorph.2004.03.004.
[70] Temmerman S, Meire P, Bouma T, Herman P, Ysebaert T, De Vriend H. Ecosystem-based coastal defence in the face of global change. Nature 2013;504:79–83. http://dx.doi.org/10.1038/nature12859.
[71] Vandenbruwaene W, Temmerman S, Bouma T, Klaassen P, de Vries M, Callaghan D, et al. Flow interaction with dynamic vegetation patches: implications for biogeomorphic evolution of a tidal landscape. J Geophys Res 2011;116:F01008. http://dx.doi.org/10.1029/2010JF001788.
[72] Wang C, Menenti M, Stoll MP, Feola A, Belluco E, M M. Separation of ground and low vegetation signatures in LiDAR measurements of salt-marsh environments. IEEE Trans Geosci Remote Sens 2009;47(7):2014–23. http://dx.doi.org/10.1109/TGRS.2008.2010490.
[73] Wang C, Temmerman S. Does bio-geomorphic feedback lead to abrupt shifts between alternative landscape states? An empirical study on intertidal flats and marshes. J Geophys Res 2013;118. http://dx.doi.org/10.1029/2012JF002474.
[74] Wang C, Wang Q, Meng Z, Meire D, Van de Koppel J, Troch P, et al. Biogeomorphic feedback between plant growth and flooding causes alternative stable state in an experimental floodplain. Adv Water Resour 2015 in press. http://dx.doi.org/10.1016/j.advwatres.2015.07.003.
[75] Wheaton JM, Gibbins C, Wainwright J, Larsen L, McElroy B. Preface: multiscale feedbacks in ecogeomorphology. Geomorphology 2011;126:265–8. http://dx.doi.org/10.1016/j.geomorph.2011.01.002.
[76] Wilson A, Evans T, Moore W, Schutte C, Joye S, Hughes A, et al. Groundwater controls ecological zonation of salt marsh macrophytes. Ecology 2015;96:840–9. http://dx.doi.org/10.1890/13-2183.1.
[77] Zedler J, Kercher S. Wetland resources: status, trends, ecosystem services, and restorability. Ann Rev Environ Resour 2005;30:39–74. http://dx.doi.org/10.1146/annurev.energy.30.050504.144248.

Please cite this article as: A. D'Alpaos, M. Marani, Reading the signatures of biologic–geomorphic feedbacks in salt-marsh landscapes, Advances in Water Resources (2015), http://dx.doi.org/10.1016/j.advwatres.2015.09.004